A novel small molecule inhibitor of MRCK prevents radiation-driven invasion in glioblastoma

Joanna L. Birch[1*], Karen Strathdee[1], Lesley Gilmour[1], Antoine Vallatos[2], Laura McDonald[3], Ariadni Kouzeli[1], Richa Vasan[1], Abdulrahman Hussain Qaisi[2], , Daniel R Croft[3], Diane Crighton[3], Kathryn Gill[3], Christopher H Gray[3], Jennifer Konczal[3], Mokdad Mezna[3], Duncan McArthur[3], Alexander W Schüttelkopf[3], Patricia McConnell[3], , Mairi Sime[3], William M. Holmes[2], Justin Bower[3], Heather J. McKinnon[3], Martin Drysdale[3], Michael F. Olson[4,5], Anthony J Chalmers[1]

[1] Wolfson Wohl Translational Cancer Research Centre, Institute of Cancer Sciences, University of Glasgow

[2]Glasgow Experimental MRI Centre, University of Glasgow

[3]CRUK Beatson Drug Discovery programme, Beatson Institute of Cancer Research, Glasgow

[4]CRUK Beatson Institute of Cancer Research, Glasgow

[5] Institute of Cancer Sciences, University of Glasgow

Running Title: Inhibition of MRCK prevents glioblastoma invasion

[*] Address for correspondence.

Dr Joanna L. Birch

Wolfson Wohl Translational Cancer Research Centre, Institute of Cancer Sciences, University of Glasgow

Joanna.birch@glasgow.ac.uk

Conflict of interest: The authors have declared that no conflict of interest exists

Abstract

Glioblastoma (GBM) is an aggressive and incurable primary brain tumour that causes severe neurological, cognitive, and psychological symptoms. Symptoms are caused and exacerbated by the infiltrative properties of GBM cells, which enable them to pervade the healthy brain and disrupt normal function. Recent research has indicated that, while radiotherapy (RT) remains the most effective component of multimodality therapy for GBM patients, it can provoke a more infiltrative phenotype in GBM cells that survive treatment. Here we demonstrate an essential role of the actin-myosin regulatory kinase myotonic dystrophy kinase-related CDC42- binding kinase (MRCK) in mediating the pro-invasive effects of radiation. MRCK-mediated invasion occurred via downstream signalling to effector molecules MYPT1 and MLC2. MRCK was activated by clinically relevant doses per fraction of radiation, and this activation was concomitant with an increase in GBM cell motility and invasion. Furthermore, ablation of MRCK activity either by RNAi or by inhibition with the novel small molecule inhibitor BDP-9066 prevented radiation-driven increases in motility both in vitro and in a clinically relevant orthotopic xenograft model of GBM. Crucially, treatment with BDP-9066 in combination with RT significantly increased survival in this model and markedly reduced infiltration of the contralateral cerebral hemisphere.

Introduction

Glioblastoma (GBM) is the most common and most aggressive primary brain tumour and is currently incurable. Poor outcomes are caused in part by the highly infiltrative nature of GBM tumour cells. This property enables them to disseminate through the brain via existing white matter tracts and perivascular spaces, making complete surgical resection unachievable and contributing to high recurrence rates. Therefore, despite aggressive treatment with surgery, radiotherapy and chemotherapy, overall survival remains extremely poor, with patients experiencing an average life expectancy of approximately one year [1]. Targeting the molecular mechanisms that underlie the invasive nature of GBM has the potential to increase survival and alleviate some of the devastating neurological disabilities associated with infiltrative disease.

The vast majority of patients with GBM receive radiotherapy as the central component of their first-line treatment. Studies in the late 1970's showed that radical radiotherapy doubles survival from approximately 6 to 12 months [2]; in 2005 a further improvement from 12 to 14 months was achieved by adding concomitant and adjuvant temozolomide to radiotherapy [1]. Every other phase III trial in this disease has been negative. It is universally accepted, therefore, that any novel therapies tested in the first-line setting must be added to a radiotherapy-based treatment schedule.

Despite its proven benefits, it is clear that radiation can also adversely affect tumour cell behaviour through alterations in cell signalling and gene expression profiles. As early as 2001, there have been studies indicating that sub-lethal doses of radiation can promote GBM cell motility and infiltration *in vitro* and *in vivo* [3, 4]. These early reports have recently been given renewed attention following the publication of a number of new studies [5-7]. The concept that radiotherapy can promote a more aggressive, infiltrative phenotype in those GBM cells that survive treatment is consistent with the repeated finding that escalating radiotherapy dose does not improve outcomes for GBM patients [8]. It also has profound implications for the development of new therapeutic avenues and highlights the need for a greater understanding of the

mechanisms that drive these changes so that new therapeutic targets can be identified and explored. For example, the failure of high radiation doses to achieve tumour control may be partly explained by tumour cells migrating outside of the irradiated volume during the treatment period.

Migration and invasion of tumour cells are driven by mechanical forces generated by changes in contractility of the actin-myosin cytoskeleton [9]. The Rho family of small GTPases comprises key regulators of actin-myosin contractility and has been widely implicated in metastasis and invasion [10, 11]. Indeed the role of RhoGTPases in GBM has been interrogated by a number of researchers, and whilst their results support a pivotal role for small GTPases and their downstream effectors, teasing out their specific contributions has proved complex, with different studies returning contradictory results [12].

RhoGTPases act via downstream effector kinases such as Rho-associated protein kinase (ROCK) and myotonic dystrophy kinase-related CDC42-binding kinase (MRCK). These downstream kinases regulate contractility of the cytoskeleton by activating phosphorylation of myosin light chain proteins (MLC) and inactivating the myosin phosphatase subunit MYPT1 to facilitate the cytoskeletal changes that are responsible for different modes of cell motility. The 'amoeboid' mode of invasion is characterised by rounded cell morphology and is highly dependent on ROCK activity [13]. Considerable effort has been invested in the development of ROCK inhibitors that could oppose RhoA driven cancer cell motility and metastasis. However, although ROCK inhibitors do indeed display strong efficacy in opposing cancer cell invasion and metastasis *in vitro* and *in vivo* [14], their clinical development has not progressed because of adverse effects on the cardiovascular system.

In contrast, mesenchymal invasion, which is classically adopted by infiltrating glioma cells, requires activity of the MRCK isoforms α and β that lie downstream of the RhoGTPase protein CDC42. This mode of invasion is characterised by an elongated cell body, actin-rich protrusions and actin-myosin contractility at the rear of the migrating cells. Unbekandt *et al* have recently demonstrated that MRCK can drive cancer cell migration, a process which can be inhibited by specific small molecule inhibitors [15-17]. Since CDC42 activity is upregulated in glioma [18, 19] and may drive the mesenchymal mode of migration employed by infiltrating glioma cells, we investigated a potential role for MRCK driven GBM cell invasion in the

pathogenesis of glioblastoma. In this study we demonstrate that MRCK activity is upregulated at the invasive edges of GBM tumours and is further enhanced by irradiation both *in vitro* and *in vivo*. We show that this response is essential to the phenomenon of radiation induced migration of GBM cells in a relevant *in vivo* model of GBM. Furthermore, by demonstrating complete abrogation of radiation driven invasion in this model using a novel small molecule inhibitor of MRCK, we confirm the pivotal role of MRCK in driving radiation induced infiltration and validate it as a novel and highly promising anti-invasive therapeutic target in GBM.

Materials and Methods

Cell culture and Radiation treatments

E2 and G7 cell lines were obtained from Colin Watts (Cambridge) and are derived from anonymized patient resection specimens as previously described [20, 21]. Cell lines were routinely cultured on Matrigel coated plates (0.23 mg/l in AdDMEM, Life Technologies) in serum free AdDMEM supplemented with 20ng/ml EGF, 10ng/ml FGF, 0.5% B27 supplement and 0.5% N2 supplement (all Life Technologies) with the exception of E2 cells for *ex vivo* migration assays which were cultured in MEM (Life Technologies) with 10% FBS. The commercially available U87MGluc2 line (Caliper Life Sciences) was cultured in MEM EBSS (Life Technologies), 10% FBS, 1% L-glutamine, 1 % NEAA (Life Technologies) and 1% NaPyruvate (Life Technologies).

Cells were irradiated using an Xstrahl RX225 radiation cabinet (195 kV X-rays, dose rate 1.39 Gy/minute).

Cell line testing

All cell lines were used in experiments between passage 2 and passage 12 from thawing and tested for mycoplasma every three months, most recent date Aug 2018. U87MGluc2 line is an authenticated cell line received from Caliper Life Sciences. E2 and G7 cell lines are primary patient-derived cell lines and as such no separate cell authentication was under taken.

Subconfluent and *ex vivo* migration assays

For subconfluent migration assays, 2 x 10^5 cells per well were plated at in 6 well dishes and migration imaged by timelapse microscopy capturing images every 15 mins. Migration velocity was calculated using single cell tracking via ImageJ analysis.

For *ex vivo* migration assays, cell were seeded onto fresh 1 mm coronal brain slices obtained from 6-8 week old C57BL/6 mice in culture medium (described above) and allowed to establish overnight with incubation at 37^{o}C, 5% CO_2. Brain slices were then inverted onto Lumox 35 mm dishes (8 µm, Sarstedt) and secured with Nuclepore Track-Etch membrane (Whatman) sealed with Matrigel. Migration was captured via confocal timelapse microscopy with images taken every 15 mins. Migration velocity was calculated using single cell tracking via ImageJ analysis.

Clonogenic assays

Cells were plated onto 6 well plates in triplicate per biological repeat. 24 hours after plating, cells were treated with DMSO or 250 µM BDP-9066 for 2 hours followed by radiation treatment and media replacement. Cells were fixed after 2-3 weeks, stained with crystal violet and colonies counted manually. Data was fitted using a linear quadratic model.

siRNA transfection and Western blotting

G7 cells were transfected with 10 nM siRNA targeting MRCKα and/or β or control scrambled siRNA (Dharmacon; MRCKα AAGAAUAUCUGCUGUGUUU, MRCKβ GAAGAAUACUGAACGAAUU, MRCKα+β CGAGAAGACUUUGAAAUAAUU) using RNAiMAX reagent (Life Technologies) and incubated for 48 hours prior to imaging or protein extraction.

For Western blotting, protein was extracted using 1% SDS/50 mM Tris pH 6.8 supplemented with protease and phosphatase inhibitors (Roche) and subject to SDS-PAGE and protein transfer. Membranes were probed using antibodies listed in supplemental table 1.

Immunofluorescence

3 x 10^3 irradiated or untreated E2 cells were plated in each well of a 96 well glass bottomed plate pre-coated with Matrigel and allowed to adhere for 2-3 hours before replacement of media with media containing DMSO or the indicated amount of BDP-9066 and incubated overnight. Cells were washed with PBS and fixed with 4% paraformaldehyde followed by permeabilisation with 0.1% TritonX/TBS. Cells were washed with TBS-Tween and blocked with 1% BSA/TBST followed by incubation with 1:200 pMLC2 antibody (Abcam cat#3675) for 1 hour at room temperature. Cells were washed and incubated with with 20 µl/ml Alexa 488 anti-mouse secondary antibody, 1:40 TR phalloidin stain, 1:300 DAPI and 1:10000 whole cell stain and incubated for 1 hr in the dark followed by final wash steps. Images were captured using the Operetta HTP microscope (Perkin Elmer) and analysis was carried out using Columbus Image Analysis software (Perkin Elmer).

Animal Studies

All animal experiments were performed under the relevant UK Home Office Project Licence and carried out with ethical approval from the University of Glasgow under the Animal (scientific Procedures) Act 1986 and the EU directive 2010. Mice were maintained in individually ventilated cages with environmental enrichment and ARRIVE guidelines followed.

Intracranial tumour model

Female CD1 nude mice were orthotopically injected with 1 x 10^5 G7 cells into the subventricular zone as previously described [20, 22]. Tumours were allowed to establish for 10-11 weeks before magnetic resonance imaging (MRI) to confirm presence of tumour. Brain irradiation was performed on an XStrahl Small Animal Radiation Research Platform (SARRP) using parallel opposed beams and a 10 x 10 mm collimator to ensure adequate tumour coverage in all animals. Mice were anaesthetised with isoflurane

and immobilised on a cradle with a tooth bar attachment. A CT scan before irradiation allowed tissue segmentation and selection of an isocentre (approx. 5mm below cell injection drill hole). Dose distributions were uniform across the brain area as shown in Fig S2C. 5mg/kg BDP-9066 or vehicle (20% propylene glycol/80% PBS) was given subcutaneously twice daily or at stated time before cull for PK analysis. Tumours were sub-dissected and fresh frozen specimens sent for PK analysis (Vertex, UK). Formalin fixed, paraffin embedded sections were stained for Ki67, HLA or phosphoMYPT1 then scanned using a Hamamatsu Nanozoomer Slide scanning machine with Leica SlidePath Slide imaging software. Algorithms were optimised for each stain individually and automated, quantitative analysis undertaken. The defining of contralateral regions was performed blinded.

MRI data acquisition and post-processing

The animals were induced in an anaesthetic chamber with 5% isoflurane and a 30:70 O_2/N_2O ratio before being transferred to the MRI instrument animal cradle allowing to monitor respiration and temperature. Imaging experiments were performed on a Bruker Biospec Avance 7 T imaging system with a 30 cm horizontal bore (Bruker, Ettlingen, German). Homogeneous radiofrequency (RF) excitation was achieved using a birdcage volume resonator (diameter 72 mm, length 110 mm) and actively decoupled 4-channel phased array receive-only head surface coils were used for signal detection, with 22 mm length for mice and 35 mm length for rats (Rapid Biomedical, Wurzburg, Germany). After standard spectrometer adjustments and geometry definition using a pilot sequence, T_2 weighted imaging was performed using a RARE sequence (Rapid Acquisition with Relaxation Enhancement); echo time=10 ms, repetition time=4,300 ms, field of view = 176x176 mm, matrix=176x176, slice thickness = 0.5 mm, 14 slices, RARE factor 8, 8 min). MRI data were the exported in DICOM format for post-processing using an in-house MATLAB code. Tumour related abnormal regions were manually selected on each T_2 slice. To evaluate tumour volumes, the number of voxels within abnormal regions was multiplied by the voxel volume.

Results

MRCK activity is upregulated at the invasive edges of GBM tumours. Oncomine analysis of MRCK gene expression in GBM revealed modest but significant upregulation of MRCKα mRNA when compared to normal brain tissue (Fig.1A, [23, 24]), suggesting a possible role in GBM pathogenesis. In light of the established role of MRCK in cancer cell motility, we explored whether its activity was spatially regulated within the tumour to support GBM cell infiltration. Indeed, using a phospho-sensitive antibody that detects MRCKalpha autophosphorylation on S1003 (pS1003) as a validated biomarker of kinase activity (pMRCK), immunohistochemical staining of matched patient tumour core and margin samples showed that positivity , and by implication MRCKalpha activity, was largely restricted to invading GBM cells at the tumour margins (Fig.1B). In support of this observation, immunohistochemical analysis of primary human tumour cells in an intracranial GBM xenograft model revealed that MYPT1, the downstream target of MRCK, also showed increased phosphorylation levels in the cytoplasm of cells at the invasive edges of the tumours (Fig.1C). These data are consistent with a role for MRCK in supporting GBM tumour cell motility and invasion.

The downstream targets of MRCK are upregulated by radiation in vitro and in vivo and this is associated with an increase in GBM invasion. Since the majority of GBM patients receive radiotherapy we explored whether MRCK activity was affected by radiation. As shown in Fig. 2A, Western blot analysis of two different primary human GBM cell lines, G7 and E2, showed that radiation induced an increase in phosphorylation levels of the MRCK biomarker, MYPT1. To confirm this observation, immunofluorescence analysis of pMLC2, another downstream biomarker of MRCK, was undertaken using a high throughput imaging platform and automated analysis (Fig.2B i, ii). This unbiased technique clearly indicated a significant increase in pMLC2 levels upon irradiation of GBM cells in vitro. Furthermore, a significant increase in the average pseudopod length was observed in irradiated cells, suggesting that the activation of MLC2 by RT is driving actin-myosin cytoskeletal changes that may promote motility (Fig. 2B iii).

To confirm that this phenomenon also occurs *in vivo*, histological staining and automated analysis of pMYPT1 levels was performed in samples from whole-brain irradiated (3 x 2Gy fractions) and non-irradiated cohorts of mice bearing intracranial G7 xenograft tumours that were sacrificed 5 days after the final radiation dose. Although no significant change in nuclear pMYPT1 was detected, we observed

significant upregulation of cytoplasmic pMYPT1 both at the invasive tumour edge (Fig. 2C i and ii) and in the tumour core (Fig. 2C iii). This suggests that MRCK activity is not only upregulated acutely, and throughout the tumour, by irradiation, but may also be maintained by a longer term 'switch' in intracellular signalling. In support of this hypothesis, analysis of tumours from smaller cohorts of mice sacrificed 12 days after the final radiation dose also showed significant upregulation of pMYPT1 (Fig. 2C iv).

Since radiation induced migration of GBM cells has recently been reported by a number of groups, and MRCK activity is known to have pro-migratory effects, we questioned whether radiation would affect cell migration. To interrogate this important question we used complementary experimental approaches in three different model systems. The invasive behaviour of cancer cells can be affected by their intrinsic ability to produce the cytoskeletal rearrangements required for forward migration as well as their ability to modify their surroundings to produce a pro-migratory environment (e.g. by degradation of extracellular matrix). Having observed a radiation induced increase in MRCK biomarkers, we first used a simple sub-confluent migration assay coupled with single cell tracking to assess whether radiation affects the intrinsic mechanisms of migration, without the complications of extracellular matrix and brain architecture (Fig.3A). These experiments showed that irradiated cells from two different primary GBM cell lines (E2 and G7) migrated significantly faster than non-irradiated cells, indicating that radiation enhances the mechanical motility of GBM cells.

To explore whether this pro-migratory effect was maintained when GBM cells have to negotiate the complexities of the brain microenvironment, we employed an *ex vivo* migration assay (fig 3B, sup. video 1 and 2). Fluorescently labelled E2 and G7 GBM cell lines were seeded onto fresh murine brain slices and their migration speed measured using confocal time-lapse microscopy and single cell tracking. We tracked >50 cells per condition encompassing all routes of invasion (i.e. perivascular and along white matter tracts) to obtain accurate average migration speeds. We observed that the average speed of cells in this assay was slower that in 2D, suggesting the brain structure poses a barrier to the invading GBM cells and that their migration in this environment requires additional processes such as extracellular matrix remodelling. However, as with the 2D migration assay, we observed that cells irradiated prior to being seeded onto the

brain slices moved significantly faster than control cells, indicating that the pro-migratory effect of radiation is maintained within the brain environment.

Finally, we demonstrated that radiation induces invasion *in vivo* by quantifying migration of GBM cells away from the primary tumour mass in control and irradiated cohorts of mice implanted with intracranial GBM xenografts (Fig. 3C). Primary human G7 GBM cells injected into the sub-ventricular zone form a tumour mass in the ipsilateral hemisphere with invasive edges. Over time, cells leave the invasive tumour edge and migrate to the contralateral hemisphere. This allows for a simple analysis of the migratory potential of tumours cells by analysing the number of tumour cells that have reached the contralateral hemisphere. To enable automated and unbiased quantification, brain sections from mice culled 17 days after initiation of radiation treatment were stained for the nuclear proliferation marker Ki67, which discriminates clearly between replicating tumour cells and the non-proliferating cells of the mouse brain (Fig. 3C i – iii). Mice had undergone T2-weighted magnetic resonance imaging (MRI) to confirm the presence and equivalence of size of tumours 11 weeks after tumour cell injection (Fig.S1 A). No effect on Ki67 staining within the tumour bulk was detected, indicating that GBM cell proliferation was unaffected by these radiation doses and would therefore not affect quantification of invading cells. In contrast, analysis of the contralateral hemisphere showed significantly higher numbers of Ki67 positive tumour cells in irradiated mice, strongly supporting the concept that radiation promotes infiltration of tumour cells to distant sites within the brain in a relevant *in vivo* mouse model. Although Ki67 staining provides a clear nuclear stain that simplifies automated analysis of histology sections, a caveat to this approach it that it would fail to detect non-proliferating GBM cells. To validate the data we also stained sections for the human Leukocyte Antigen (HLA Class I ABC). We found that Ki67 and HLA staining correlated well (Fig. S1 B), and observed increased numbers of HLA positive cells in the contralateral hemispheres of the irradiated cohort, confirming the observations made with Ki67 (Fig. 3C iii).

MRCK plays an essential role in driving radiation induced migration. To probe whether increased cell migration requires enhanced MRCK activity, and to assess its relative contribution, we performed subconfluent migration assays in G7 cells in which MRCKα and β had been downregulated by siRNA

targeting (Fig.4A and B). Ablation of both MRCK isoforms concomitantly was found to inhibit pMYPT1 expression and to reduce migration speed to the levels observed in non-irradiated control cells. These findings strongly indicate that MRCK, and not ROCK, is primarily responsible for the downstream signalling to MYPT1 and MLC2 that drives radiation induced migration in GBM cells.

Specific targeting of MRCK, but not ROCK, using a novel small molecule inhibitor, does not affect cell survival but elicits a robust biomarker and motility dose response at sub-micromolar concentrations. We have developed a novel small molecule inhibitor, BDP-9066, that displays high selectivity towards MRCKα/β over related kinases such as ROCK ([17], Fig.4C, Supp. Table 2). BDP-9066 demonstrates excellent selectivity for MRCKα and MRCKβ over the closely related kinases ROCK1 and ROCK2. Furthermore, BDP-9066 also shows excellent selectivity when screened in a larger kinase panel (1μM BDP-9066 against 113 kinases; 7/113 kinases show inhibition >80%, [17]). The biochemical activity and selectivity of BDP-9066 was maintained in cellular assays.

To test whether BDP-9066 had any impact on tumour cell survival either as a single agent or in combination with radiation we performed cell viability and clonogenic survival assays. No effect on viability was observed at sub-micromolar levels of BDP-9066 (Fig.4C i), and 250 nM BDP-9066 had no impact on the radiation sensitivity of G7 or E2 cells as measured by clonogenic survival (Fig.4 ii) despite compound being in excess of the IC50 indicated in Fig 4D i. The loss of cell viability at higher concentrations is likely to represent off target toxicity. Confirmation that BDP-9066 is inhibiting its target is provided by the robust dose response of the MRCK biomarker pMLC2 in irradiated GBM cells as measured by immunofluorescence (IC50 = 56nM; Fig. 3D i). The response of non-irradiated GBM cells to the inhibitor was highly variable, suggesting a lack of synchronicity of MRCK activity in unirradiated cells. In contrast, when we tested BDP-9066 in our *in vitro* and *ex vivo* migration assays we found that the compound completely blocked the radiation induced increase in cell motility observed in subconfluent migration assays at a concentration of 100nM (Fig. 4E). This anti-invasive activity of BDP-9066 was also confirmed using the organotypic *ex vivo* brain slice assay (Fig. 4F). Further experiments showed a robust dose response of irradiated cells to BDP-9600 in subconfluent migration assays (Fig. 4G i). Importantly, treatment with the ROCK specific inhibitor

Y27632 did not inhibit migration of irradiated cells (Fig. 4G ii), providing further evidence that the pro-invasive effect of RT is primarily driven through MRCK activation.

Pharmacological inhibition of MRCK inhibits radiation induced infiltration by GBM cells in vivo. Compound level analysis of sub dissected intracranial U87MG and G7 tumours indicated that BDP-9066 penetrated intracranial tumours at concentrations that would be expected to inhibit of MRCK *in vivo*, even when adjusted for free drug levels (based on plasma protein binding of 27.3%; Fig. 5A). Samples taken from the contralateral hemisphere showed that BDP-9066 has very low exposure in the brain in the absence of significant tumour burden, following subcutaneous dosing. To test the efficacy of BDP-9066 in inhibiting radiation induced invasion *in vivo* we established G7 intracranial tumours in four cohorts of mice: vehicle, BDP-9066, RT + vehicle and RT + BDP-9066. Mice underwent T2-weighted MRI to confirm the presence and equivalence of size of tumours 11 weeks after tumour cell injection (Fig. S2A); treatment was commenced the following week. Mice in the RT cohorts received 3 x 2Gy whole brain RT over the course of one week (Fig S2 B). Twice daily dosing of vehicle or BDP-9066 was initiated at the same time as RT and continued for 10 days before sacrifice of the animals to ensure sustained inhibition of MRCK (Fig. 5B). Twice daily dosing was chosen because, while the pharmacokinetic (PK) profile of BDP-9066 showed good bioavailability, rapid clearance was also observed [17]. The compound was well tolerated and PK analysis of blood taken at the time of culling confirmed its presence at micromolar concentrations (Fig. S2 C). A transient vasodilatory effect lasting 20 - 30 minutes was noted in some animals as evidenced by reddening of the ears.

Mouse brains were excised and subjected to immunohisochemical analysis of Ki67 staining. Consistent with our previous experiment, increased numbers of GBM cells were observed in the contralateral hemispheres of mice in the 'irradiated + vehicle' cohort (Fig.5C). Importantly, irradiated mice that were treated with BDP-9066 showed no increase of tumour cell infiltration to the contralateral hemisphere. These data confirm that BDP-9066 prevents radiation induced infiltration of GBM *in vivo*. Immunohistological staining for the MRCK biomarker pMYPT1 (Fig. 5C ii) showed reduced expression in the RT + BDP-9066 cohort compared to RT + vehicle, indicating that the anti-invasive effects of the inhibitor are likely 'on target'.

BDP-9066 induces an aberrant morphology through the disruption of the actin-myosin cytoskeleton in GBM cells. In vitro and *ex vivo* timelapse imaging of cells treated with BDP-9066 revealed the emergence of an aberrant morphology characterised by increased numbers of neurite-like structures emanating from the cell body that appeared to prevent migration (Sup. video 3 -6). To characterise this further, high throughput imaging was performed on irradiated E2 cells in which the actin cytoskeleton had been stained with fluorescently labelled phalloidin (Fig.6A). Cells treated with BDP-9066 exhibited a highly disordered cytoskeletal structure, indicating that MRCK inhibition disrupts normal actin-myosin dynamics, leading to the aberrant morphology and reduced migratory potential observed. To explore this further, automated analysis was undertaken to measure the number of neurite roots in response to escalated doses of BDP-9066 in both irradiated and untreated cells (Fig.6B). Neurite numbers increased in a dose dependent manner under both conditions, but as with the pMLC2 biomarker response (Fig. 4D), data from non-irradiated cells was highly variable compared to irradiated cells. This provides further evidence that radiation synchronises MRCK activity across the cell population, rendering more cells sensitive to inhibition by BDP-9066 and eliciting a more uniform and more striking response.

Treatment with BDP-9066 significantly increases survival in a pre-clinical model of GBM. To assess whether inhibiting the invasive capacity of GBM cells *in vivo* confers a survival benefit, we performed an extended efficacy experiment using the G7 intracranial tumour model (fig. 7A). Tumours were allowed to establish for 9 weeks before the mice underwent T2-weighted MRI to establish tumour establishment and enable randomisation of mice into cohorts, stratified by tumour size. Treatment commenced at week 10 on mice randomised into 4 cohorts: no RT + vehicle, no RT + BDP-9066, RT + vehicle and RT + BDP-9066. RT was fractionated into 6 x 2Gy over two weeks. BDP-9066 or vehicle (blinded) was administered twice daily, Monday- Friday, for a total of four weeks (two weeks concomitant with and two weeks adjuvant after RT). Treatment was limited to 4 weeks under veterinary guidance to reduce the stress of repeat dosing on the animals. Mice were culled upon presentation of clinical symptoms (weight loss, seizures, tilting etc). Only mice that were culled after the first week of treatment were included in the survival analysis to provide adequate time for treatment to take effect. The experiment was terminated at 104 days after T2 weighted MRI scans had been performed on the remaining mice.

The results clearly indicate that, while RT alone provided a survival benefit, this was significantly enhanced when combined with BDP-9066, despite the inhibitor only being administered for a restricted period of time (Fig. 7B). Additionally, although quantitation of contralateral invasion could not be applied in this experiment as the mice were culled at varying time points, histological analysis indicates that tumours from the RT + BDP-9066 cohort are more contained with less invasive margins than RT + vehicle cohort (Fig. 7C). Indeed qualitative assessment of invasion extent showed that 8 out of 14 RT + vehicle mice showed extensive contralateral invasion compared to only 3 out of 13 RT+ BDP-9066 mice. The variation in cull time also means that any potential effect on tumour size could not be assessed in this experiment as mice were culled at clinical endpoint and thereby all likely to be carrying a significant tumour burden. These data provide important evidence that adding a novel MRCK targeting, anti-invasive small molecule treatment to radiation therapy has the potential to improve outcomes in this cancer of unmet need by negating the adverse, pro-invasive effects of radiation.

Discussion

Glioblastoma is the most aggressive primary brain tumour in adults and the least responsive to treatment. These adverse clinical features are partly attributable to the infiltrative nature of the disease. Glioblastoma cells undergo a number of biological and morphological changes that allow them to migrate through the perivascular spaces and white matter tracts of the brain. The role that RhoGTPases and their effector kinases play in these processes have been interrogated by a number of researchers [12], and inhibition of CDC42, the upstream activator of MRCK, has been shown to inhibit migration of glioma cells [25-27]. However, little is known about the effects of ionising radiation on these pathways and the subsequent downstream effects on migration and invasion. In addition, by augmenting actin-myosin cytoskeleton plasticity through targeting the upstream regulator MRCK, we are hitting a regulatory node that is a convergence point for a number of signalling pathways that have previously shown to be important in GBM invasion such as integrin and FAK signalling [28] [29, 30].

Analysis of MRCK gene expression using Oncomine datasets indicated that, whilst expression is raised in tumour samples compared to the normal brain, this increase is modest. We postulated that overall gene

expression levels might fail to reflect more pronounced upregulation at the tumour margins, where increased MRCK activity may be required to support tumour cell infiltration of the healthy brain tissue. Such spatial restriction of gene expression has been documented for other pro-migratory factors such as EGFR [31, 32]. By measuring MRCK-specific auto-phosphorylation at Ser1003 in patient derived tumour core and tumour margin samples we observed that MRCK activity is indeed specifically upregulated in infiltrating GBM cells, indicating an important influence of this signalling pathway on invasion. Furthermore we demonstrated that exposure to radiation further increases MRCK signalling to drive increased migration both *in vitro* and in a clinically relevant intracranial GBM tumour model. Interestingly, this radiation induced activation of MRCK extended into the tumour core whereas in the absence of radiation MRCK activation biomarkers were observed only at the tumour margin. This indicates that MRCK activation by RT is not restricted to cells at the tumour margin and therefore may have potential to drive other biological processes within the tumour core.

The question of whether radiation promotes the invasive behaviour of GBM cells has been controversial for many years. However, recent publications from a number of research groups [5-7] and the data presented here provide robust evidence in support of this phenomenon and highlight the potential value of incorporating anti-invasive strategies into standard first line therapy for GBM. While the observation that most glioblastomas recur within the maximally irradiated volume [33-35] has been used as an argument against radiation induced invasion being of clinical relevance, an alternative explanation is that local tumour recurrence is caused by repopulation of the irradiated tumour bed by tumour cells from outside the irradiated volume. Evidence for repopulation of laser ablated regions of tumour by GBM cells was recently presented by Osswald *et al* [36] and may represent a novel and important mechanism of treatment resistance. Such a model also is supported by the observation that a significant proportion of tumours recur at the periphery of the irradiated volume [33]. This mechanism of tumour recurrence would require surviving GBM cells to retain their invasive capacity and would also be consistent with the well documented failure of radiation dose escalation to either reduce tumour recurrence rates or reduce the incidence of recurrence within the irradiated volume [8, 37, 38].

Our data support the theory that novel anti-invasive chemotherapeutics for GBM should always be evaluated in the context of radiotherapy, not only because of the pro-invasive effects of radiation, but also to ensure that candidate compounds are active against tumour cells whose signalling pathways have been fundamentally altered by radiotherapy. Our results show that, while ablation of MRCK activity effectively inhibited the migration and infiltration of irradiated cells, there was a reduced effect on non-irradiated control cells *in vitro* and *in vivo*. Furthermore, our results indicate that radiation induced effects on glioblastoma cells *in vivo* are not transient but can persist for days after the conclusion of radiotherapy.

Our study utilised a novel, highly specific inhibitor of MRCK, BDP-9066 that was developed in-house by the CRUK Beatson Drug Discovery Programme. Treating primary GBM cells with this compound *in vitro* revealed that MRCK inhibition induces a highly aberrant morphology characterised by disordered, neurite-like protrusions. Not only do these morphological changes appear to prevent GBM cells from migrating persistently, they may have additional implications for GBM biology and resistance to therapy. Winkler *et al* recently published an elegant study that identified a network of communicating glioma cell protrusions, termed 'tumour microtubes (TM)', which contributed to chemo- and radioresistance *in vivo* [36, 39-41]. Since TM formation is highly dependent on cytoskeletal dynamics and BDP-9066 specifically induces aberrant protrusions, it is possible that MRCK inhibition will exert therapeutic effects *in vivo* by disrupting the TM communication network.

As part of our *in vivo* studies we demonstrated that BDP-9066 penetrates intracranial tumours in two different mouse models of GBM at levels that far exceeded the biomarker IC_{50} values calculated for irradiated GBM cell lines. Drug levels in the contralateral hemisphere were much lower, reflecting limited penetration of the intact blood-brain barrier, which may be of value in protecting normal brain cells and reducing toxicity. Conversely, delivery of BDP-9066 to regions of low tumour cell density may be compromised by limited BBB disruption, although evidence exists that suggest that focal disruption of the BBB can be elicited by single invading glioma cells [42]. To maximize efficacy it may be advantageous to develop the current series of compounds to include a more BBB penetrant molecule that would penetrate areas of very low tumour burden. Most importantly, our results demonstrate conclusively that BDP-9066

completely blocks the pro-invasive effects of radiation on GBM cells, preventing them from disseminating to intracranial sites distant from the primary tumour; this effect translated in to a survival benefit when BDP-9066 was given in combination with RT.

As mentioned previously, the development of effective ROCK inhibitors for clinical use has been hindered by severe adverse effects on the cardiovascular system. Although we observed a mild vasodilatory effect in some animals, to date, we have no evidence that MRCK inhibition would elicit a similarly intolerable response to ROCK inhibition, but such a possibility should be carefully considered during optimisation of MRCK specific compounds for clinical use.

This study did not extend to investigating the combination of BDP-9066 in combination with both RT and temozolomide (TMZ). SInce TMZ is a component of standard of care for GBM patients it will be important to determine whether it modulates the interaction between RT and MRCK inhibition as this novel treatment strategy progresses towards the clinic.

In conclusion, our data provides novel and persuasive evidence that delivery of BDP-9066 or a related compound alongside radiotherapy has potential not only to extend survival of patients with GBM, but also to improve the devastating neurological symptoms associated with these infiltrative tumours.

Acknowledgements

This work was funded by a grant awarded by The Brain Tumour Charity (grant ref. number 26/160; JBirch, AChalmers, KStrathdee, LGilmore, AVallatos) and in part by Cancer Research UK (MDrysdale, JBower, HMckinnon, LMacDonald, DCroft, KGill, CGray, JKonczal, MMezna, DMcArthur, ASchüttelkopf, PMcConnell, MSime) and the Beatson Endowment Fund (JLB). Primary GBM cell lines and patient GBM tumour samples were obtained from Colin Watts, Cambridge.

References

1. Stupp R, Mason WP, van den Bent MJ, Weller M, Fisher B, Taphoorn MJ, Belanger K, Brandes AA, Marosi C, Bogdahn U *et al*: **Radiotherapy plus concomitant and adjuvant temozolomide for glioblastoma**. *N Engl J Med* 2005, **352**(10):987-996.

2. Walker MD, Alexander E, Jr., Hunt WE, MacCarty CS, Mahaley MS, Jr., Mealey J, Jr., Norrell HA, Owens G, Ransohoff J, Wilson CB *et al*: **Evaluation of BCNU and/or radiotherapy in the treatment of anaplastic gliomas. A cooperative clinical trial**. *J Neurosurg* 1978, **49**(3):333-343.
3. Wild-Bode C, Weller M, Rimner A, Dichgans J, Wick W: **Sublethal irradiation promotes migration and invasiveness of glioma cells: implications for radiotherapy of human glioblastoma**. *Cancer Res* 2001, **61**(6):2744-2750.
4. Zhai GG, Malhotra R, Delaney M, Latham D, Nestler U, Zhang M, Mukherjee N, Song Q, Robe P, Chakravarti A: **Radiation enhances the invasive potential of primary glioblastoma cells via activation of the Rho signaling pathway**. *J Neurooncol* 2006, **76**(3):227-237.
5. Edalat L, Stegen B, Klumpp L, Haehl E, Schilbach K, Lukowski R, Kuhnle M, Bernhardt G, Buschauer A, Zips D *et al*: **BK K+ channel blockade inhibits radiation-induced migration/brain infiltration of glioblastoma cells**. *Oncotarget* 2016, **7**(12):14259-14278.
6. Kegelman TP, Wu B, Das SK, Talukdar S, Beckta JM, Hu B, Emdad L, Valerie K, Sarkar D, Furnari FB *et al*: **Inhibition of radiation-induced glioblastoma invasion by genetic and pharmacological targeting of MDA-9/Syntenin**. *Proceedings of the National Academy of Sciences of the United States of America* 2017, **114**(2):370-375.
7. Xiong Y, Ji W, Fei Y, Zhao Y, Wang L, Wang W, Han M, Tan C, Fei X, Huang Q *et al*: **Cathepsin L is involved in X-ray-induced invasion and migration of human glioma U251 cells**. *Cellular signalling* 2017, **29**:181-191.
8. Lee SW, Fraass BA, Marsh LH, Herbort K, Gebarski SS, Martel MK, Radany EH, Lichter AS, Sandler HM: **Patterns of failure following high-dose 3-D conformal radiotherapy for high-grade astrocytomas: a quantitative dosimetric study**. *International journal of radiation oncology, biology, physics* 1999, **43**(1):79-88.
9. Hall A: **The cytoskeleton and cancer**. *Cancer metastasis reviews* 2009, **28**(1-2):5-14.
10. Bishop AL, Hall A: **Rho GTPases and their effector proteins**. *The Biochemical journal* 2000, **348 Pt 2**:241-255.
11. Pandya P, Orgaz JL, Sanz-Moreno V: **Modes of invasion during tumour dissemination**. *Molecular oncology* 2017, **11**(1):5-27.
12. Khalil BD, El-Sibai M: **Rho GTPases in primary brain tumor malignancy and invasion**. *J Neurooncol* 2012, **108**(3):333-339.
13. Croft DR, Olson MF: **Regulating the conversion between rounded and elongated modes of cancer cell movement**. *Cancer cell* 2008, **14**(5):349-351.
14. Rath N, Olson MF: **Rho-associated kinases in tumorigenesis: re-considering ROCK inhibition for cancer therapy**. *EMBO reports* 2012, **13**(10):900-908.
15. Unbekandt M, Croft DR, Crighton D, Mezna M, McArthur D, McConnell P, Schuttelkopf AW, Belshaw S, Pannifer A, Sime M *et al*: **A novel small-molecule MRCK inhibitor blocks cancer cell invasion**. *Cell communication and signaling : CCS* 2014, **12**:54.
16. Unbekandt M, Olson MF: **The actin-myosin regulatory MRCK kinases: regulation, biological functions and associations with human cancer**. *Journal of molecular medicine* 2014, **92**(3):217-225.
17. Unbekandt M, Belshaw S, Bower J, Clarke M, Cordes J, Crighton D, Croft DR, Drysdale MJ, Garnett MJ, Gill K *et al*: **Discovery of Potent and Selective MRCK Inhibitors with Therapeutic Effect on Skin Cancer**. *Cancer Res* 2018, **78**(8):2096-2114.
18. Tysnes BB, Mahesparan R: **Biological mechanisms of glioma invasion and potential therapeutic targets**. *Journal of neuro-oncology* 2001, **53**(2):129-147.
19. Alonso MM, Diez-Valle R, Manterola L, Rubio A, Liu D, Cortes-Santiago N, Urquiza L, Jauregi P, Lopez de Munain A, Sampron N *et al*: **Genetic and epigenetic modifications of Sox2 contribute to the invasive phenotype of malignant gliomas**. *PloS one* 2011, **6**(11):e26740.
20. Ahmed SU, Carruthers R, Gilmour L, Yildirim S, Watts C, Chalmers AJ: **Selective Inhibition of Parallel DNA Damage Response Pathways Optimizes Radiosensitization of Glioblastoma Stem-like Cells**. *Cancer research* 2015, **75**(20):4416-4428.
21. Fael Al-Mayhani TM, Ball SL, Zhao JW, Fawcett J, Ichimura K, Collins PV, Watts C: **An efficient method for derivation and propagation of glioblastoma cell lines that conserves the molecular profile of their original tumours**. *Journal of neuroscience methods* 2009, **176**(2):192-199.

22. Gomez-Roman N, Stevenson K, Gilmour L, Hamilton G, Chalmers AJ: **A novel 3D human glioblastoma cell culture system for modeling drug and radiation responses**. *Neuro-oncology* 2017, **19**(2):229-241.
23. Bredel M, Bredel C, Juric D, Harsh GR, Vogel H, Recht LD, Sikic BI: **Functional network analysis reveals extended gliomagenesis pathway maps and three novel MYC-interacting genes in human gliomas**. *Cancer research* 2005, **65**(19):8679-8689.
24. Bredel M, Bredel C, Juric D, Harsh GR, Vogel H, Recht LD, Sikic BI: **High-resolution genome-wide mapping of genetic alterations in human glial brain tumors**. *Cancer research* 2005, **65**(10):4088-4096.
25. Yiin JJ, Hu B, Jarzynka MJ, Feng H, Liu KW, Wu JY, Ma HI, Cheng SY: **Slit2 inhibits glioma cell invasion in the brain by suppression of Cdc42 activity**. *Neuro-oncology* 2009, **11**(6):779-789.
26. Furukawa K, Kumon Y, Harada H, Kohno S, Nagato S, Teraoka M, Fujiwara S, Nakagawa K, Hamada K, Ohnishi T: **PTEN gene transfer suppresses the invasive potential of human malignant gliomas by regulating cell invasion-related molecules**. *International journal of oncology* 2006, **29**(1):73-81.
27. Malchinkhuu E, Sato K, Horiuchi Y, Mogi C, Ohwada S, Ishiuchi S, Saito N, Kurose H, Tomura H, Okajima F: **Role of p38 mitogen-activated kinase and c-Jun terminal kinase in migration response to lysophosphatidic acid and sphingosine-1-phosphate in glioma cells**. *Oncogene* 2005, **24**(44):6676-6688.
28. Reyes SB, Narayanan AS, Lee HS, Tchaicha JH, Aldape KD, Lang FF, Tolias KF, McCarty JH: **αvβ8 integrin interacts with RhoGDI1 to regulate Rac1 and Cdc42 activation and drive glioblastoma cell invasion**. *Mol Biol Cell* 2013, **24**(4):474-482.
29. Webb DJ, Donais K, Whitmore LA, Thomas SM, Turner CE, Parsons JT, Horwitz AF: **FAK-Src signalling through paxillin, ERK and MLCK regulates adhesion disassembly**. *Nat Cell Biol* 2004, **6**(2):154-161.
30. Kwiatkowska A, Kijewska M, Lipko M, Hibner U, Kaminska B: **Downregulation of Akt and FAK phosphorylation reduces invasion of glioblastoma cells by impairment of MT1-MMP shuttling to lamellipodia and downregulates MMPs expression**. *Biochim Biophys Acta* 2011, **1813**(5):655-667.
31. Snuderl M, Fazlollahi L, Le LP, Nitta M, Zhelyazkova BH, Davidson CJ, Akhavanfard S, Cahill DP, Aldape KD, Betensky RA *et al*: **Mosaic amplification of multiple receptor tyrosine kinase genes in glioblastoma**. *Cancer cell* 2011, **20**(6):810-817.
32. Okada Y, Hurwitz EE, Esposito JM, Brower MA, Nutt CL, Louis DN: **Selection pressures of TP53 mutation and microenvironmental location influence epidermal growth factor receptor gene amplification in human glioblastomas**. *Cancer research* 2003, **63**(2):413-416.
33. Weber DC, Casanova N, Zilli T, Buchegger F, Rouzaud M, Nouet P, Vees H, Ratib O, Dipasquale G, Miralbell R: **Recurrence pattern after [(18)F]fluoroethyltyrosine-positron emission tomography-guided radiotherapy for high-grade glioma: a prospective study**. *Radiotherapy and oncology : journal of the European Society for Therapeutic Radiology and Oncology* 2009, **93**(3):586-592.
34. Chen L, Chaichana KL, Kleinberg L, Ye X, Quinones-Hinojosa A, Redmond K: **Glioblastoma recurrence patterns near neural stem cell regions**. *Radiotherapy and oncology : journal of the European Society for Therapeutic Radiology and Oncology* 2015, **116**(2):294-300.
35. Minniti G, Amelio D, Amichetti M, Salvati M, Muni R, Bozzao A, Lanzetta G, Scarpino S, Arcella A, Enrici RM: **Patterns of failure and comparison of different target volume delineations in patients with glioblastoma treated with conformal radiotherapy plus concomitant and adjuvant temozolomide**. *Radiotherapy and oncology : journal of the European Society for Therapeutic Radiology and Oncology* 2010, **97**(3):377-381.
36. Osswald M, Jung E, Sahm F, Solecki G, Venkataramani V, Blaes J, Weil S, Horstmann H, Wiestler B, Syed M *et al*: **Brain tumour cells interconnect to a functional and resistant network**. *Nature* 2015, **528**(7580):93-98.
37. Fitzek MM, Thornton AF, Rabinov JD, Lev MH, Pardo FS, Munzenrider JE, Okunieff P, Bussiere M, Braun I, Hochberg FH *et al*: **Accelerated fractionated proton/photon irradiation to 90 cobalt gray equivalent for glioblastoma multiforme: results of a phase II prospective trial**. *Journal of neurosurgery* 1999, **91**(2):251-260.
38. Chan JL, Lee SW, Fraass BA, Normolle DP, Greenberg HS, Junck LR, Gebarski SS, Sandler HM: **Survival and failure patterns of high-grade gliomas after three-dimensional conformal**

radiotherapy. *Journal of clinical oncology : official journal of the American Society of Clinical Oncology* 2002, **20**(6):1635-1642.
39. Osswald M, Solecki G, Wick W, Winkler F: **A malignant cellular network in gliomas: potential clinical implications**. *Neuro-oncology* 2016, **18**(4):479-485.
40. Weil S, Osswald M, Solecki G, Grosch J, Jung E, Lemke D, Ratliff M, Hanggi D, Wick W, Winkler F: **Tumor microtubes convey resistance to surgical lesions and chemotherapy in gliomas**. *Neuro-oncology* 2017.
41. Winkler F: **Tumour network in glioma**. *ESMO open* 2016, **1**(6):e000133.
42. Watkins S, Robel S, Kimbrough IF, Robert SM, Ellis-Davies G, Sontheimer H: **Disruption of astrocyte-vascular coupling and the blood-brain barrier by invading glioma cells**. *Nat Commun* 2014, **5**:4196.

Figure 1. MRCK activity is upregulated at the invasive edge of GBM tumours. (A) Oncomine analysis of data from two separate studies indicating increased MRCKα mRNA expression in clinical GBM samples compared to normal brain tissue. **(B)** Matched tumour margin and tumour core samples were obtained from patients with GBM and stained for an MRCK activity auto-phosphorylation site, S1003. Cytplasmic pMRCK levels were quantified using automated analysis on SlidePath. Statistical analysis: two tailed, unpaired t test. N.S. = not significant, ** $p < 0.01$. **(C)** Example image from samples obtained from a G7 intracranial tumour mouse model stained for pMYPT1, a downstream target of MRCK.

Figure 2. MRCK activity is stimulated by radiation *in vitro* and *in vivo* (A) Two primary cell lines, E2 and G7, were treated with 0, 2 or 5 Gy and protein lysates extracted after 24 hours. Western blot analysis was undertaken to assay levels of pMYPT1. Actin and tubulin were used as loading controls and γ-H2AX as a marker of radiation induced DNA damage. **(B)** (i) E2 cells were treated with 0 or 2 Gy and stained by immunofluorescence for pMLC2. Cells were imaged using an Operetta high-throughput imaging platform. Green: pMLC2; yellow: actin; red: whole cell dye; blue: DAPI; Final panel: merge. Scale bar: 100µm. (ii) Automated image analysis was undertaken to compare pMLC2 levels in control and irradiated cells. (iii) Pseudopod length was quantified using automated image analysis. Data are derived from two biological repeats, each analysing >400 cells per condition. Statistical analysis: two tailed, unpaired t test. **** $p < 0.0001$ **(C)** Cohorts of mice bearing G7 intracranial tumours were subjected to 3 x 2Gy fractions of whole brain irradiation or left untreated. Brain sections were stained by IHC for pMYPT1 levels (i). (ii), (iii) Levels of nuclear and cytoplasmic pMYPT1 were quantified in mice sacrificed 5 days post RT. (iv) Levels of cytoplasmic pMYPT1 were measured 12 days post RT. Quantification was done via automated analysis using SlidePath ; n = 5 (no RT) and 6 (3 x 2 Gy), 5 day timepoint; n = 4 (no RT) and 4 (3 x 2 Gy), 12 day time point . Scale bar: 100µm. Statistical analysis: two tailed, unpaired t test. N.S. = not significant, * $p < 0.05$.

Figure 3. Activation of MRCK by radiation is concomitant with increased motility of GBM cells *in vitro* and *in vivo*. (A) E2 and G7 were treated with 0 or 2Gy and their motility analysed in a sub-confluent migration assay using time-lapse microscopy and single cell tracking. (i) Example track plots of individual control and irradiated E2 cells imaged over 16 hours, 15 min intervals. (ii) Comparison of control and irradiated cell speed. **(B)** Fluorescently labelled E2 or G7 cells were irradiated with 2Gy or left untreated and seeded onto fresh murine brain slices. Cell motility was analysed using confocal time-lapse microscopy (i). (ii) Cell speed was measured using single cell tracking. Data from 3 biological replicates. Scale bar: 50μm Statistical analysis: Mann-Whitney test, ** $p < 0.005$, **** $p < 0.0001$. **(C)** (i) Brain sections from control and irradiated mice bearing G7 intracranial tumours were stained via IHC for Ki67 to indicate presence of cycling GBM tumour cells. (ii) % Ki67 positive cells in the tumour bulk were quantified using automated analysis in specimens from mice culled 10 days after initiation of treatment; n = 6 in both cohorts. The percentage of Ki67 positive cells (iii) or HLC (iv) in the contralateral hemisphere of mice culled 17 days after initiation of treatment was quantified using automated image analysis. Scale bar: 1mm. Statistical analysis: two tailed, unpaired t test. N.S. = not significant, ** $p < 0.005$.

Figure 4. Inhibition of MRCK activity opposes radiation driven motility but does not affect cell survival *in vitro*. (A) G7 cells were transfected with siRNAs targeting MRCKα and MRCKβ, alone or in combination. (i) Cell lysates were analysed by Western blotting for MRCKα, MRCKβ and pMYPT1 levels. (ii) Treated cells were exposed to 0Gy or 2Gy and imaged in a sub-confluent migration assay. Cell speed was measured by single cell tracking. Statistical analysis: Mann-Whitney test, N.S. = not significant, *< p 0.05, ** $p < 0.005$, *** $p < 0.001$. **(B)** Novel MRCK specific inhibitor, BDP-9066. **(C)** (i) Cell viability assays performed on G7 cells treated with increasing concentrations of BDP-9066;d data plotted relative to vehicle control. (ii) Clonogenic survival assays performed on G7 and E2 cells irradiated in the presence of vehicle or 0.25 μM BDP-9066. N.S. = not significant. **(D)** E2 cells treated with 2 Gy radiation (i) or untreated (ii) in the presence of increasing amounts of BDP-9066, and stained by immunofluorescence for pMLC2. Cells were imaged using an Operetta high-throughput imaging platform. Automated image analysis was used to compare pMLC2 levels. Data from two biological repeats with >400 cells per condition per biological replicate. Data plotted as a percentage of vehicle. **(E)** E2 and G7 cells were exposed to 0 Gy or 2 Gy radiation in the presence of DMSO or BDP-9066 and cell speed measured in a subconfluent migration assay using timelapse microscopy and single cell tracking. Data from 3 biological replicates. **(F)** Fluorescently labelled E2 cells were exposed to 0 Gy or 2 Gy radiation and seeded onto fresh murine brain slices. Cell motility was assayed in the presence of DMSO or BDP-9066 by confocal timelapse microscopy and single cell tracking using ImageJ. Data from 3 biological replicates. For all *in vitro* and *ex vivo* motility assays statistical analysis was performed using Mann-Whitney test: N.S. = not significant, *< p 0.05, ** $p < 0.005$, *** $p < 0.001$, ****$p <$ 0.0001. **(G)** E2 and G7 cells were exposed to 2 Gy in the presence of increasing amounts of BDP-9066 (i) or

Y-27632 followed by timelapse microscopy and single cell tracking. Data from 3 biological replicates. Baseline speed was calculated to be 34 from the measurement of >20 non-migratory cells.

Figure 5. BDP-9066 penetrates intracranial GBM xenografts and inhibits radiation induced infiltration of GBM cells *in vivo*. (A) Mice bearing U87MG (i) or G7 (ii) intracranial tumours were injected subcutaneously with 5 mg/Kg BDP-9066 30 mins prior to cull. Tumours were sub-dissected from normal brain tissue and analysed by mass spectrometry to determine total compound levels ('Total'). These levels were adjusted using a determined PPB free value of 72.7 % to estimate available BDP-9066 levels in the tumours ('Free'); n = 4 (U87MG) and 10 (G7); CL = contralateral. **(B)** Outline of experiment to measure *in vivo* GBM cell response to BDP-9066. G7 intracranial tumours were allowed to establish for 12 weeks before initiation of treatment. **(C)** Cohorts of mice from **(B)** were culled and excised brains subjected to IHC for Ki67 followed by automated analysis to determine extent of contralateral hemisphere invasion by GBM cells.

Figure 6. BDP-9066 treatment disrupts the actin-myosin cytoskeleton inducing an aberrant morphology that inhibits migration. (A) (i) E2 cells were exposed to 0 or 2 Gy radiation in the presence of DMSO or BDP-9066. Cells were imaged using an Operetta high-throughput imaging platform. Red: actin, blue: DAPI, Scale bar: 100µm. (ii) Automated image analysis was undertaken to quantify changes in neurite morphology. Data from > 1000 cells. **(B)** Radiation stimulates MRCK activity, activating MLC2 and driving actin-myosin contractility and subsequent cell migration. Treatment with BDP-9066 inhibits MRCK activity resulting in a disrupted actin-myosin cytoskeleton and loss of motility.

Figure 7. Combining BDP-9066 with RT confers a significant survival advantage on mice bearing intracranial GBM tumours. (A) Outline of experiment to measure *in vivo* survival to BDP-9066 treatment. G7 intracranial tumours were allowed to establish for 10 weeks before initiation of treatment. Mice in the RT cohorts received 6 x 2Gy whole brain RT over the course of two weeks. Only mice that were culled after the first 3 fractions of RT were included in the analysis to allow for any treatment benefit to take effect. The study was randomised, blinded and the mice stratified across the cohorts based on starting tumour size as assessed by T2 MRI. **(B)** Kaplan-Meier plot showing survival data. N.S. = not significant, *< p 0.05, ** p < 0.005. Statistical analysis: Log-rank (Mantel-Cox) test. **(C)** Example histology from RT + vehicle and RT + BDP-9066 cohorts

Figure 1

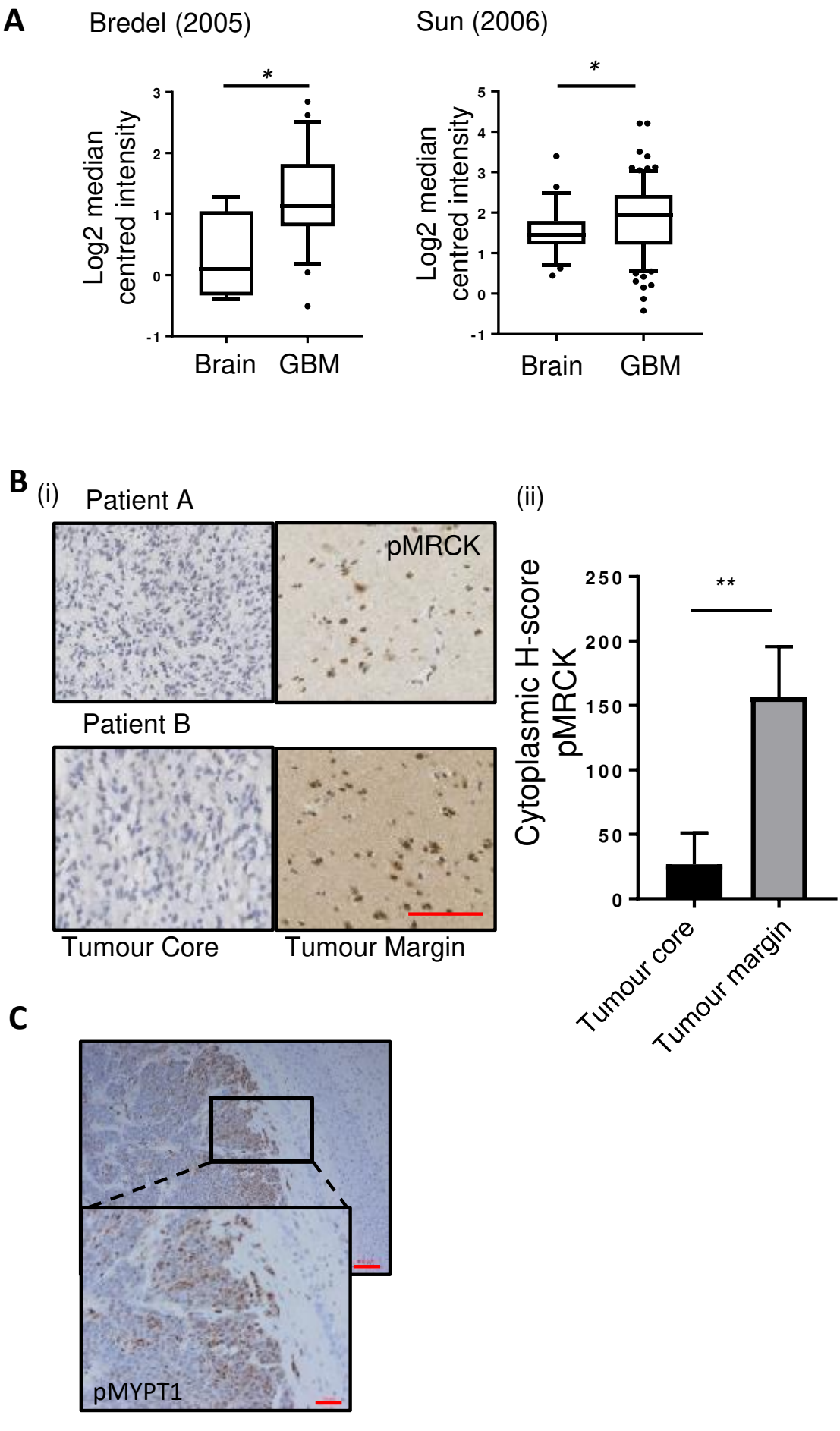
A
Bredel (2005)
Sun (2006)
Log2 median centred intensity
Brain
GBM
B
(i)
Patient A
pMRCK
Patient B
Tumour Core
Tumour Margin
(ii)
Cytoplasmic H-score pMRCK
Tumour core
Tumour margin
C
pMYPT1

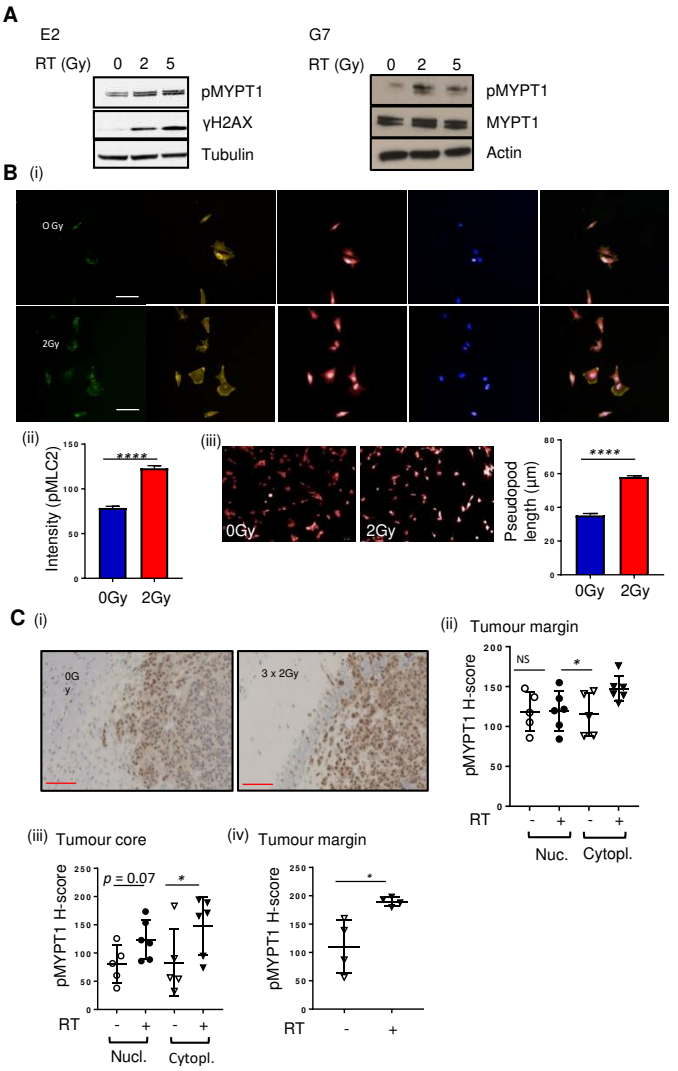
A
E2
RT (Gy) 0 2 5
pMYPT1
γH2AX
Tubulin
G7
RT (Gy) 0 2 5
pMYPT1
MYPT1
Actin
B (i)
0 Gy
2Gy
(ii)
Intensity (pMLC2)
****
0Gy 2Gy
(iii)
0Gy
2Gy
Pseudopod length (μm)
****
0Gy 2Gy
C (i)
0G y
3 x 2Gy
(ii) Tumour margin
pMYPT1 H-score
NS
*
RT
- + - +
Nuc. Cytopl.
(iii) Tumour core
pMYPT1 H-score
p = 0.07
*
RT
- + - +
Nucl. Cytopl.
(iv) Tumour margin
pMYPT1 H-score
*
RT
- +

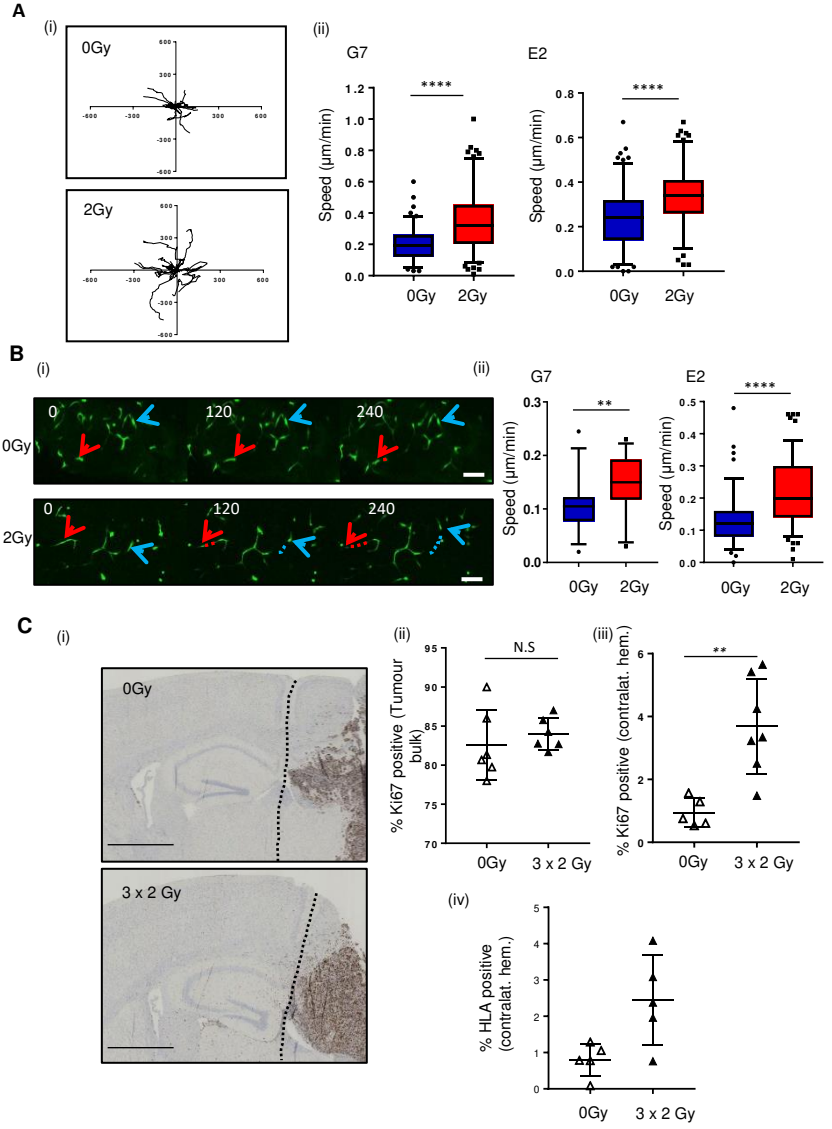
A
(i)
0Gy
2Gy
(ii)
G7
E2
Speed (µm/min)
****
0Gy
2Gy
B
(i)
0
120
240
0Gy
2Gy
(ii)
G7
E2
Speed (µm/min)
**
****
0Gy
2Gy
C
(i)
0Gy
3 x 2 Gy
(ii)
% Ki67 positive (Tumour bulk)
N.S
0Gy
3 x 2 Gy
(iii)
% Ki67 positive (contralat. hem.)
**
0Gy
3 x 2 Gy
(iv)
% HLA positive (contralat. hem.)
0Gy
3 x 2 Gy

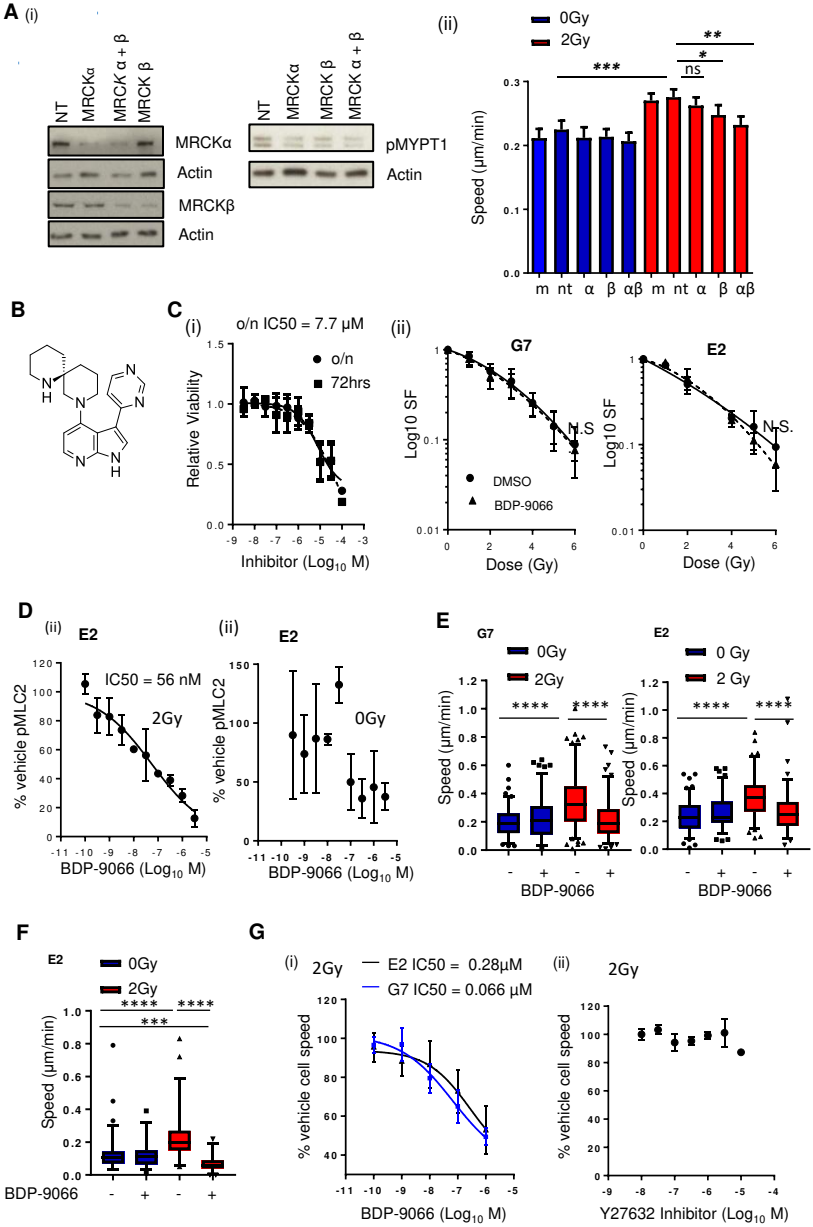
A (i)
NT
MRCKα
MRCK α + β
MRCK β
MRCKα
Actin
MRCKβ
Actin
NT
MRCKα
MRCK β
MRCK α + β
pMYPT1
Actin
(ii)
0Gy
2Gy
***
**
*
ns
Speed (μm/min)
m nt α β αβ m nt α β αβ
B
C
(i)
o/n IC50 = 7.7 μM
o/n
72hrs
Relative Viability
Inhibitor (Log10 M)
(ii)
G7
E2
Log10 SF
N.S
DMSO
BDP-9066
Dose (Gy)
D
(ii) E2
IC50 = 56 nM
2Gy
% vehicle pMLC2
BDP-9066 (Log10 M)
(ii) E2
0Gy
% vehicle pMLC2
BDP-9066 (Log10 M)
E
G7
E2
0Gy
2Gy
Speed (μm/min)
****
BDP-9066
F
E2
0Gy
2Gy
****
***
Speed (μm/min)
BDP-9066
G
(i) 2Gy
E2 IC50 = 0.28μM
G7 IC50 = 0.066 μM
% vehicle cell speed
BDP-9066 (Log10 M)
(ii) 2Gy
% vehicle cell speed
Y27632 Inhibitor (Log10 M)

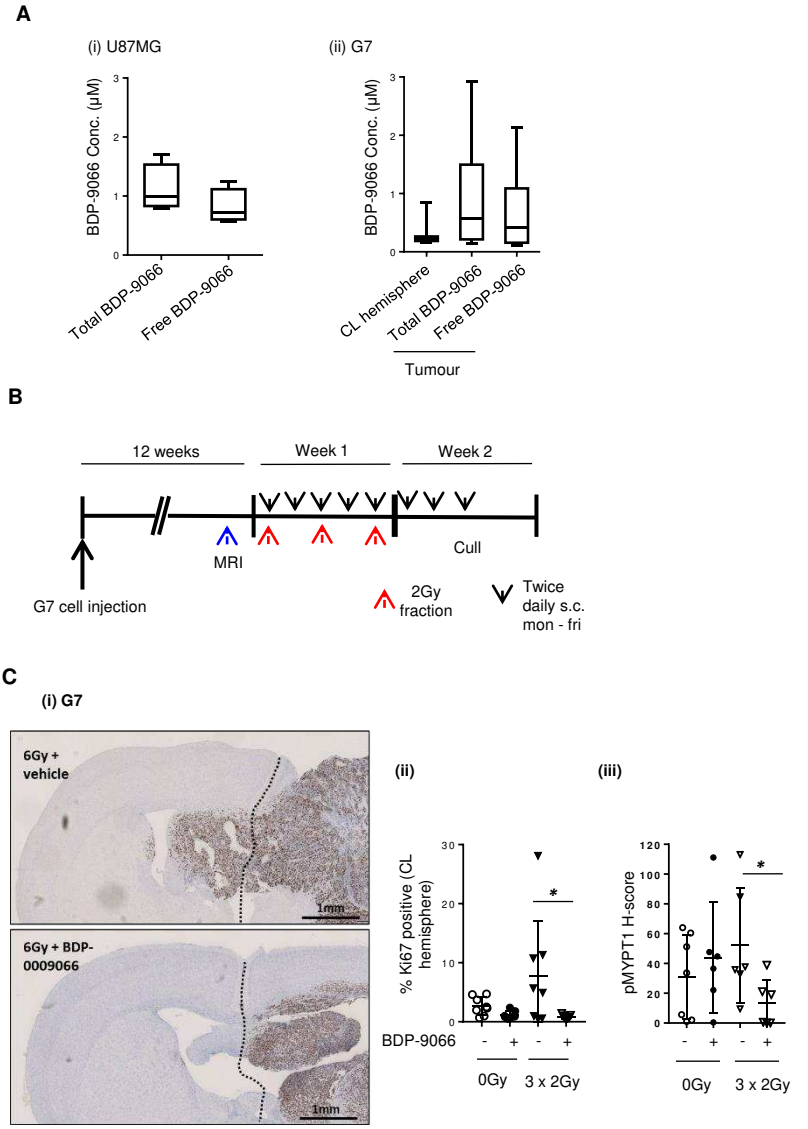
A
(i) U87MG
(ii) G7
BDP-9066 Conc. (μM)
Total BDP-9066
Free BDP-9066
CL hemisphere
Tumour
B
12 weeks
Week 1
Week 2
MRI
Cull
G7 cell injection
2Gy fraction
Twice daily s.c. mon - fri
C
(i) G7
6Gy + vehicle
6Gy + BDP-0009066
1mm
(ii)
(iii)
% Ki67 positive (CL hemisphere)
pMYPT1 H-score
BDP-9066
0Gy
3 x 2Gy

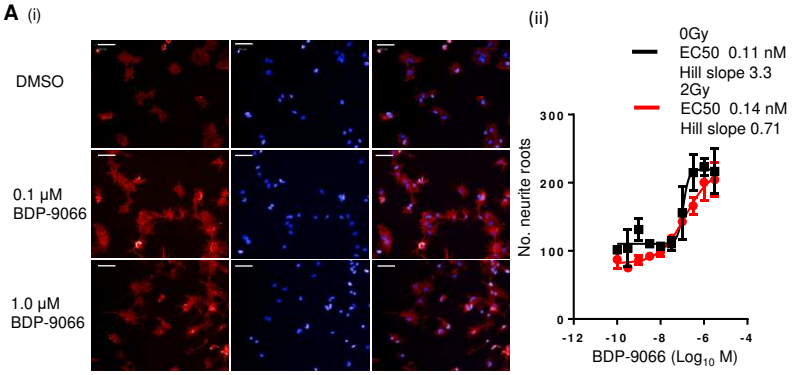
A (i)
DMSO
0.1 μM BDP-9066
1.0 μM BDP-9066
(ii)
0Gy
EC50 0.11 nM
Hill slope 3.3
2Gy
EC50 0.14 nM
Hill slope 0.71
No. neurite roots
300
200
100
0
-12
-10
-8
-6
-4
BDP-9066 (Log10 M)

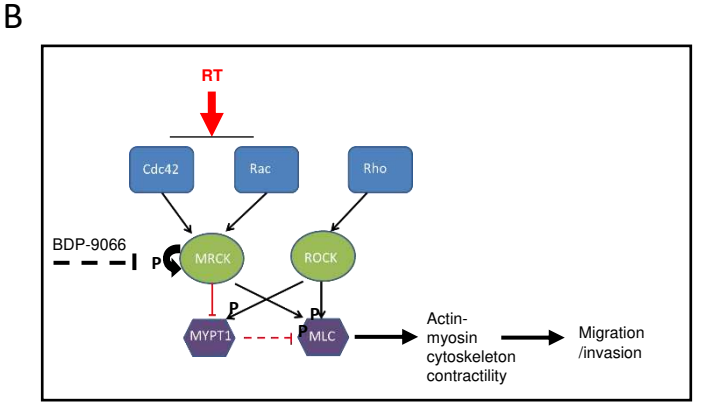
B
RT
Cdc42
Rac
Rho
BDP-9066
P
MRCK
ROCK
P
P
MYPT1
P
MLC
Actin-myosin cytoskeleton contractility
Migration /invasion

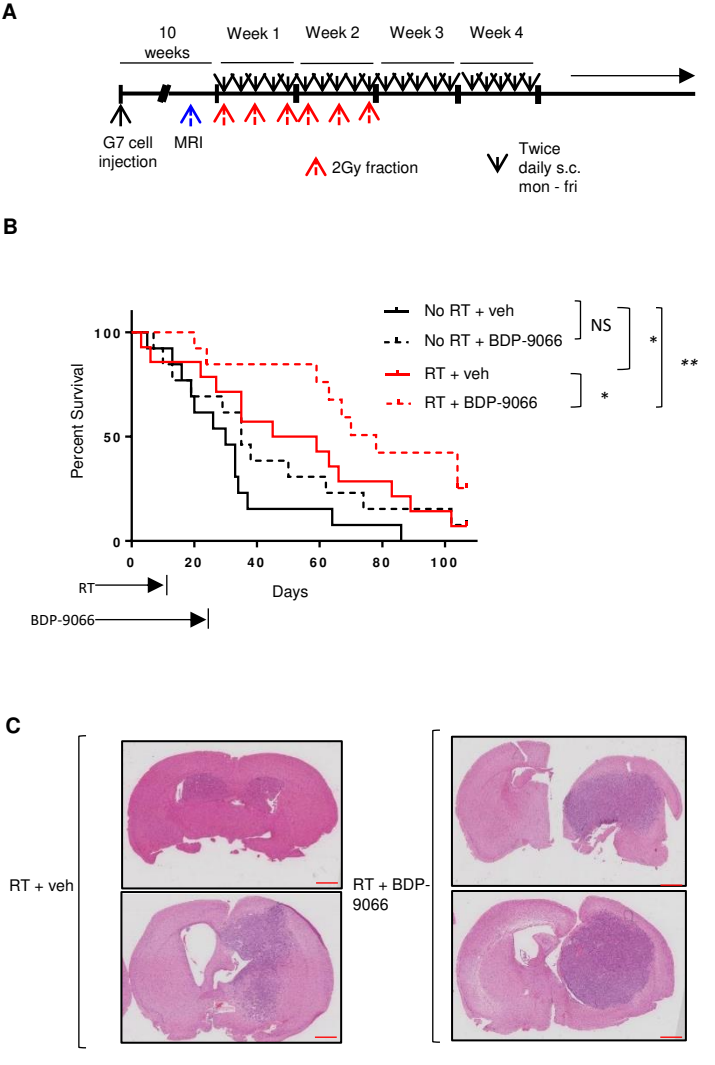
A
10 weeks
Week 1
Week 2
Week 3
Week 4
G7 cell injection
MRI
2Gy fraction
Twice daily s.c. mon - fri
B
No RT + veh
No RT + BDP-9066
RT + veh
RT + BDP-9066
NS
*
**
*
Percent Survival
100
50
0
0
20
40
60
80
100
Days
RT
BDP-9066
C
RT + veh
RT + BDP-9066